Laryngoscope
Investigative Otolaryngology

ORIGINAL RESEARCH OPEN ACCESS

# Development of a Clinical Prediction Model to Predict Malignant Transformation of Sinonasal Inverted Papilloma Based on Hematological Indices and Clinical Features

Kai Sun[1] | Ce Wu[1] | Zengxiao Zhang[1] | Jiahong Chen[2] | Xudong Yan[1] | Shunke Li[1] | Lin Wang[1] | Longgang Yu[1] | Yan Jiang[1]

[1]Department of Otolaryngology, Head and Neck Surgery, The Affiliated Hospital of Qingdao University, Qingdao, China | [2]Department of Otolaryngology, Qingdao Women and Children's Hospital, Qingdao, China

**Correspondence:** Longgang Yu (yulonggang@qdu.edu.cn) | Yan Jiang (jiangyanoto@qdu.edu.cn)

**Received:** 5 September 2024 | **Revised:** 17 December 2024 | **Accepted:** 24 December 2024

**Funding:** This work was supported by National Natural Science Foundation of China, 81770978.

**Keywords:** cytokeratin fragment antigen 21-1 | malignant transformation | nomogram | sinonasal inverted papilloma

## ABSTRACT

**Objective:** Sinonasal inverted papilloma (SNIP) has a risk of malignant transformation into SNIP with squamous cell carcinoma (SNIP-SCC). Early detection of SNIP-SCC is crucial for patient outcomes. This study aimed to evaluate the utility of tumor-related hematological indices in the early diagnosis of SNIP-SCC and to develop a nomogram incorporating imaging and clinical features.

**Methods:** This study included 159 patients with SNIP with ($n = 34$) or without ($n = 125$) SCC. Univariate and multivariate logistic regression analyses were employed to identify independent risk factors and develop nomogram. The diagnostic model was evaluated using receiver operating characteristics (ROC), standard, clinical decision, and clinical impact curves.

**Results:** Elevated serum cytokeratin fragment antigen 21-1 (CYFRA 21-1), the loss of convoluted cerebriform pattern, bone destruction, headache/facial pain, and epistaxis/blood-tinged mucus were identified as independent risk factors for SNIP-SCC. The optimal cut-off value for serum CYFRA 21-1 was 3.51 ng/mL, with the nomogram area under the ROC curve of 0.966 based on the above indicators.

**Conclusion:** The findings suggest that CYFRA 21-1 is a promising diagnostic marker for SNIP-SCC. The nomogram incorporating serum CYFRA 21-1, imaging features, and clinical factors demonstrates strong clinical utility and can be a reference tool for clinical decision-making.

## 1 | Introduction

Sinonasal inverted papilloma (SNIP) is a common benign nasal sinus tumor originating from the Schneiderian nasal epithelium, comprising 0.5%–4% of nasal sinus tumors, with a 7%–10% risk of malignant transformation into squamous cell carcinoma (SNIP-SCC) [1–3]. Malignant transformation of SNIP significantly impacts prognosis and complicates management, requiring more aggressive surgical resection to reduce the high risk of recurrence. Therefore, timely and accurate preoperative diagnosis is crucial for effective treatment of SNIP-SCC [4–7].

Several clinical methods are available for the early diagnosis of SNIP-SCC, with local biopsy being the most widely used

Kai Sun and Ce Wu contributed equally to this study.

diagnostic approach. However, the malignant transformation of SNIP may not involve the entire tumor, resulting in the inability to accurately obtain a malignant tumor tissue sample [8–10]. Imaging modalities such as CT and MRI are also used, but their specificity can be limited as SNIP-SCC appears as apparent bone destruction on CT [11] and SNIP also has a similar presentation [12, 13]. The convoluted cerebriform pattern (CCP) is a typical and distinctive MRI feature of SNIP [14–16] and its absence may indicate the malignant transformation of SNIP [17]. However, the clinical use of MRI is limited in patients with implanted pacemakers, metallic and internally fixed metals, therapeutic pumps, and those with claustrophobia [18]. Moreover, some primary care facilities may lack the necessary equipment for comprehensive patient evaluation, contributing to misdiagnosis and delayed diagnosis. Consequently, early identification and differential diagnosis of SNIP-SCC and SNIP remain challenging.

Blood indices are readily available clinical markers linked to the diagnosis, treatment, and prognosis of various tumors. Traditional tumor-related serum markers, such as cytokeratin fragment antigen 21-1 (CYFRA 21-1) and serum squamous cell carcinoma antigen (SCCA), have demonstrated diagnostic value in SNIP [19, 20]. Recent research has also highlighted the importance of novel serum markers, including systemic inflammatory and nutritional markers, in tumorigenesis and progression [21, 22]. However, these tumor-related blood markers remain understudied in SNIP-SCC.

Therefore, this study aimed to evaluate the diagnostic utility of tumor-related hematological indicators for SNIP-SCC. To differentiate SNIP-SCC from SNIP at an early stage, we developed a column-line diagram-based diagnostic model incorporating these indicators and patient clinical characteristics. This model aims to provide a novel reference tool for clinical practice.

## 2 | Methods

### 2.1 | Study Population

This single-center retrospective study was approved by the Medical Ethics Committee of Qingdao University Affiliated Hospital. All participants provided written informed consent. A review of our center's pathology database identified 125 patients with SNIP and 34 patients with SNIP-SCC who underwent surgical treatment between August 2019 and May 2024. All patients met the diagnostic criteria outlined in the European Position Paper on Endoscopic Treatment of Nasal, Sinus, and Skull Base Tumors (2010). The inclusion criteria included: (1) patients with postoperative pathological diagnosis of SNIP or SNIP-SCC; (2) patients with a complete collection of tumor-related blood indices within 7 days preoperatively; and (3) patients with complete clinical data. The exclusion criteria included: (1) patients with fungal or odontogenic maxillary sinusitis; (2) patients with other sinus diseases such as combined sinus cysts, cystic fibrosis, cilia motility disorders, or other sinus tumors; (3) patients with immunodeficiency; and (4) patients with concurrent or previous history of other tumors.

### 2.2 | Data Collection

Clinical data collected included sex, age, height, weight, body mass index (BMI), smoking dependence, alcohol dependence history, nasal symptoms (nasal obstruction, runny nose, headache/facial pain, rhinorrhea/blood in the runny nose, and decreased sense of smell), history of sinus surgery, pathological diagnosis, and imaging data (bone destruction and bone hyperplasia in CT and the CCP in MRI). Laboratory parameters required for the study, including SCCA, CYFRA 21-1, albumin, prealbumin, globulin, neutrophil count, lymphocyte count, and platelet count, were also collected at least 1 week before surgery.

### 2.3 | Nutritional and Systemic Inflammatory Indices

The following formulae were used to calculate the nutritional and systemic inflammatory indices for the study: neutrophil-to-lymphocyte ratio (NLR) = neutrophils/lymphocytes; platelet-to-lymphocyte ratio (PLR) = platelets/lymphocytes; albumin-to-globulin ratio (AGR) = albumin/globulin; nutritional inflammatory index (ALI) = BMI × albumin/globulin; Prognostic Nutritional Inflammation Index (PNI) = albumin + 0.005 × lymphocytes; Signs of Immunoinflammation Index (SII) = platelets × neutrophils/lymphocytes.

### 2.4 | Sinus CT and MRI

All patients underwent preoperative sinus CT scanning using Siemens Somatomplus4 and GEHiSpeedNX/iCT scanners. Sinus CT was primarily used to evaluate the extent of sinus lesions and any associated bone hyperplasia or destruction. MRI examinations were conducted using a GESignaHDxt3.0TMRI scanner with an eight-channel phased array head coil. Conventional MRI scanning was performed, and the MRI evaluation index was the CCP. CCP refers to parallel strips of high and low signals within the tumor.

### 2.5 | Statistical Methods

Statistical analyses were performed using the Statistical Package for Social Sciences version 26.0 (IBM, Corp, Armonk, NY, USA) and the R software version 4.1.3 (R Foundation, Vienna, Austria). Normally distributed quantitative data were expressed as mean ± standard deviation ($\bar{x} \pm s$) and compared using the Student's *t*-test. Non-normally distributed quantitative data were expressed as median ± interquartile range ($M \pm Q_R$) and compared using the Mann–Whitney *U* test. Qualitative indicators were expressed as frequencies and proportions and compared using the chi-square or Fisher's exact tests. Independent risk factors for SNIP-SCC were identified using univariate and multivariate logistic regression analyses, and the odds ratios (OR) and 95% confidence intervals (CI) were calculated. Diagnostic models were developed using column line plots, and the diagnostic power of the model was evaluated using receiver operating characteristics (ROC) curves and calibration curves. All statistical tests were two-tailed, and statistical significance was considered at $p < 0.05$.

## 3 | Result

### 3.1 | Baseline Data of the Study Population

A total of 159 patients were included: 115 males and 44 females, with an average age of 56.18 ± 11.47 years. Patients were categorized into two groups based on malignant transformation: 34 with SNIP-SCC and 125 with SNIP only. Detailed patient characteristics are presented in Table 1. The SNIP-SCC group exhibited significantly higher rates of headache/facial pain ($p < 0.001$), epistaxis/blood-tinged mucus ($p < 0.001$), and history of sinus surgery ($p < 0.001$) compared to the SNIP-only group. Additionally, there were similar significant differences between the two groups in age serum CYFRA 21-1 levels, nutritional indicators, and systemic inflammation indicators of PNI ($p < 0.001$), ALI ($p < 0.001$), NLR ($p = 0.006$), PLR ($p = 0.007$), and SII ($p = 0.001$). For imaging characteristics, the incidence of bone destruction ($p < 0.001$) and hyperplasia ($p = 0.005$) on CT and CCP ($p < 0.001$) in MRI

**TABLE 1** | Baseline characteristics of the study participants ($n = 159$).

| Variables | SNIP ($n = 125$) | SNIP-SCC ($n = 34$) | $p$ |
|---|---|---|---|
| Age, years (mean ± SD) | 55.26 ± 12.32 | 59.53 ± 6.68 | 0.115 |
| Gender | | | 0.860 |
| Male | 90 (72.00%) | 25 (73.53%) | |
| Female | 35 (28.00%) | 9 (26.47%) | |
| BMI, kg/m$^2$ (mean ± SD) | 24.57 ± 4.89 | 23.75 ± 3.86 | 0.123 |
| Smoking dependence | 42 (33.60%) | 17 (50%) | 0.079 |
| Alcohol dependence | 36 (28.80%) | 15 (44.12%) | 0.090 |
| History of sinus surgery | 22 (17.60%) | 18 (52.94%) | < 0.001 |
| Nasal symptoms | | | |
| Nasal obstruction | 114 (91.20%) | 27 (79.41%) | 0.054 |
| Runny nose | 70 (56.00%) | 14 (41.18%) | 0.125 |
| Reduction or loss of smell | 64 (51.20%) | 13 (38.24%) | 0.180 |
| Epistaxis/blood-tinged mucus | 32 (25.60%) | 20 (58.82%) | < 0.001 |
| Headache/facial pain | 35 (28.00%) | 23 (67.65%) | < 0.001 |
| Blood indices | | | |
| SCCA (median ± IQR) | 3.90 ± 5.39 | 6.50 ± 10.11 | 0.095 |
| CYFRA 21-1 (median ± IQR) | 2.39 ± 1.43 | 4.07 ± 2.36 | < 0.001 |
| AGR (median ± IQR) | 1.26 ± 0.27 | 1.53 ± 0.20 | 0.061 |
| PNI (median ± IQR) | 44.40 ± 3.66 | 41.48 ± 3.15 | < 0.001 |
| NLR (median ± IQR) | 2.98 ± 1.45 | 2.58 ± 1.91 | 0.006 |
| PLR (median ± IQR) | 121.74 ± 53.46 | 143.27 ± 74.50 | 0.007 |
| ALI (median ± IQR) | 563.06 ± 418.76 | 352.21 ± 337.45 | < 0.001 |
| SII (median ± IQR) | 482.31 ± 384.43 | 642.19 ± 607.15 | 0.001 |
| Imaging characteristics | | | |
| Bone destruction | 30 (24.00%) | 33 (97.06%) | < 0.001 |
| Bone hyperplasia | 103 (82.40%) | 22 (64.70%) | 0.026 |
| CCP | | | < 0.001 |
| None | 24 (19.20%) | 19 (55.88%) | |
| Partial | 25 (20.00%) | 10 (29.41%) | |
| Diffuse | 76 (60.80%) | 5 (14.71%) | |

Abbreviations: AGR, albumin to globulin ratio; ALI, advanced lung cancer inflammation index; BMI, body mass index; CCP, Convoluted Cerebriform Patterning; CYFRA 21-1, cytokeratin fragment antigen 21-1; IQR, interquartile range; NLR, neutrophil-to-lymphocyte ratio; PLR, platelet-to-lymphocyte ratio; PNI, prognostic nutritional index; SCCA, squamous cell carcinoma antigen; SD, standard deviation; SII, systemic immune-inflammation index; SNIP, sinonasal inverted papillomas; SNIP-SCC, sinonasal inverted papilloma with squamous cell carcinoma.

were significantly higher in the SNIP-SCC group than in the SNIP-only group. No significant differences were observed for gender ($p=0.860$), age ($p=0.115$), nasal obstruction ($p=0.054$), reduction or loss of smell ($p=0.180$), runny nose (0.125), smoking dependence ($p=0.079$), alcohol dependence ($p=0.090$), SCCA ($p=0.095$), BMI ($p=0.123$), and AGR ($p=0.061$).

### 3.2 | Univariate and Multivariate Logistic Regression

Univariate logistic regression analyses revealed that serum CYFRA 21-1 (OR = 1.923, 95% CI, 1.434–2.577, $p<0$ 0.001), PNI (OR = 0.803, 95% CI, 0.717–0.899, $p<0$ 0.001), ALI (OR = 0.997, 95% CI, 0.996–0.999, $p=0$ 0.001), headache/facial pain (OR = 5.377, 95% CI, 2.373–12.180, $p<0$ 0.001), epistaxis/blood-tinged mucus (OR = 4.152, 95% CI, 1.880–9.170, $p<0$ 0.001), a history of sinus surgery (OR = 5.267, 95% CI, 2.330–11.908, $p<0.001$), bone destruction (OR = 104.500, 95% CI, 13.706–796.741, $p<0.001$), and bone hyperplasia (OR = 0.305, 95% CI, 0.134–0.695, $p=0.005$) in CT, disappearance of the CCP in MRI (OR = 0.111, 95% CI, 0.038–0.322, $p<0.001$) were significantly associated with SNIP-SCC (Table 2).

Multivariate logistic regression analysis identified serum CYFRA 21-1 (OR = 1.900, 95% CI, 1.496–2.736, $p=0.043$), headache/facial pain (OR = 7.796, 95% CI, 1.346–45.164, $p=0.022$), epistaxis/blood-tinged mucus (OR = 7.093, 95% CI, 1.381–36.415, $p=0.019$), disappearance of the CCP in MRI (OR = 0.127, 95% CI, 0.017–0.963, $p=0.046$), and bone destruction in CT(OR = 84.245, 95%CI, 6.431–1103.536, $p=0.001$) as independent risk factors for SNIP-SCC (Table 3).

**TABLE 2** | Univariate logistic regression analysis for identification of factors associated with SNIP-SCC.

| Variables | β | Se | Wald | OR | 95% CI | p |
|---|---|---|---|---|---|---|
| Age | 0.035 | 0.019 | 3.632 | 1.036 | (0.999–1.074) | 0.057 |
| Gender | −0.234 | 0.451 | 0.270 | 0.791 | (0.327–1.914) | 0.603 |
| BMI | −0.066 | 0.049 | 1.783 | 0.936 | (0.850–1.031) | 0.182 |
| Smoking dependence | 0.681 | 0.392 | 3.023 | 1.976 | (0.917–4.259) | 0.082 |
| Alcohol dependence | 0.669 | 0.398 | 2.825 | 1.952 | (0.895–4.257) | 0.093 |
| History of sinus surgery | 1.661 | 0.416 | 15.936 | 5.267 | (2.330–11.908) | <0.001 |
| Nasal symptoms | | | | | | |
| Nasal obstruction | −0.988 | 0.529 | 3.494 | 0.372 | (0.132–1.049) | 0.062 |
| Runny nose | −0.598 | 0.392 | 2.322 | 0.550 | (0.255–1.187) | 0.128 |
| Reduction or loss of smell | −0.528 | 0.396 | 1.778 | 0.590 | (0.272–1.281) | 0.182 |
| Epistaxis/blood-tinged mucus | 1.424 | 0.404 | 12.399 | 4.152 | (1.880–9.170) | <0.001 |
| Headache/facial pain | 1.682 | 0.417 | 16.254 | 5.377 | (0.373–12.180) | <0.001 |
| Blood indices | | | | | | |
| SCCA | 0.018 | 0.014 | 1.711 | 1.018 | (0.991–1.046) | 0.191 |
| CYFRA 21-1 | 0.705 | 0.154 | 20.955 | 2.023 | (1.496–2.736) | <0.001 |
| AGR | −1.481 | 0.798 | 3.445 | 0.227 | (0.048–1.087) | 0.063 |
| PNI | −0.219 | 0.058 | 14.368 | 0.803 | (0.717–0.899) | <0.001 |
| NLR | 0.152 | 0.089 | 2.928 | 1.164 | (0.717–0.899) | 0.087 |
| PLR | 0.003 | 0.003 | 1.728 | 1.003 | (0.998–1.008) | 0.189 |
| ALI | −0.003 | 0.001 | 10.651 | 0.997 | (0.996–0.999) | 0.001 |
| SII | 0.001 | <0.001 | 3.355 | 1.001 | (1.000–1.001) | 0.067 |
| Imaging characteristics | | | | | | |
| Bone destruction | 4.649 | 1.036 | 20.123 | 104.500 | (13.706–796.741) | <0.001 |
| Bone hyperplasia | −0.938 | 0.429 | 4.778 | 0.392 | (0.169–0.908) | 0.029 |
| CCP | −1.183 | 0.255 | 21.520 | 0.306 | (0.186–0.505) | <0.001 |

Abbreviations: β, slope parameter; AGR, albumin to globulin ratio; ALI, advanced lung cancer inflammation index; BMI, body mass index; CCP, Convoluted Cerebriform Patterning; CI, confidence interval; CYFRA 21-1, cytokeratin fragment antigen 21-1; NLR, neutrophil-to-lymphocyte ratio; OR, odds ratio; PLR, platelet-to-lymphocyte ratio; PNI, prognostic nutritional index; SCCA, squamous cell carcinoma antigen; Se, standard error; SII, systemic immune-inflammation index.

**TABLE 3** | Multivariate logistic regression analysis for identification of factors associated with SNIP-SCC.

| Variables | *β* | Se | Wald | OR | 95% CI | *p* |
|---|---|---|---|---|---|---|
| Epistaxis/blood-tinged mucus | 1.959 | 0.835 | 5.509 | 7.093 | (1.381–36.415) | 0.019 |
| Headache/facial pain | 2.054 | 0.896 | 5.250 | 7.796 | (1.346–45.164) | 0.022 |
| History of sinus surgery | 1.579 | 0.891 | 3.140 | 4.848 | (0.846–27.782) | 0.076 |
| CYFRA 21-1 | 0.642 | 0.317 | 4.088 | 1.900 | (1.020–3.540) | 0.043 |
| PNI | −0.149 | 0.123 | 1.482 | 0.861 | (0.678–1.095) | 0.223 |
| ALI | −0.001 | 0.002 | 0.434 | 0.999 | (0.996–1.002) | 0.510 |
| Bone destruction | 4.434 | 1.313 | 11.411 | 84.245 | (6.431–1103.536) | 0.001 |
| Bone hyperplasia | −2.012 | 1.060 | 3.604 | 0.134 | (0.017–1.067) | 0.058 |
| CCP | −2.063 | 1.034 | 3.984 | 0.127 | (0.017–0.963) | 0.046 |

Abbreviations: *β*, slope parameter; ALI, advanced lung cancer inflammation index; CCP, Convoluted Cerebriform Patterning; CI, confidence interval; CYFRA 21-1, cytokeratin fragment antigen 21-1; OR, odds ratio; PNI, prognostic nutritional index; Se, standard error.

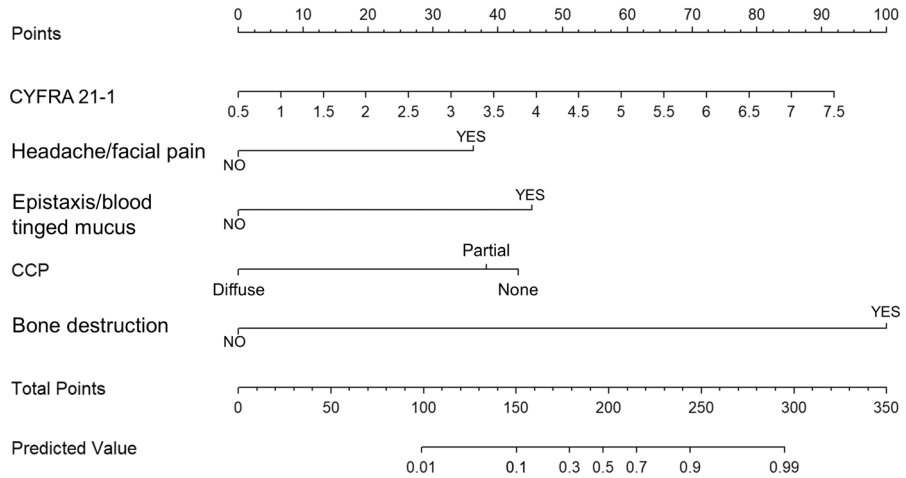


**FIGURE 1** | Nomogram for predicting the malignant transformation into sinonasal inverted papilloma with squamous cell carcinoma. CCP, Convoluted Cerebriform Patterning; CYFRA 21-1, cytokeratin fragment antigen 21-1.

### 3.3 | Nomogram Construction and Validation

A diagnostic model was developed using nomogram based on the multivariate logistic regression analysis results (Figure 1). In the nomogram model, a vertical line was drawn from the corresponding point on the scale of each variable to the highest scale, and a score was assigned. The individual variable scores were summed to obtain a total score, and a vertical line was drawn from the corresponding position on the total score scale to the lowest score to predict the risk of SNIP-SCC. Bone destruction was the most influential variable in the model, followed by CYFRA 21-1, epistaxis/blood-tinged mucus, loss of CCP, and headache/facial pain. The area under the curve (AUC) of the nomogram was 0.966 (0.95% CI, 0.936–997), indicating excellent predictive power (Figure 2A). The calibration curve demonstrated good agreement between the model and actual outcomes, suggesting that the model was well-calibrated (Figure 2B). The decision curve analysis (DCA) indicated that patients could benefit from the model (Figure 2C). Furthermore, the clinical impact curves showed the strong clinical applicability of the column-line diagram model in predicting SNIP-SCC (Figure 2D).

### 3.4 | Discussion

SNIP-SCC patients require a more aggressive treatment approach, including extensive preoperative planning, intraoperative resection, and postoperative adjuvant therapies like radiotherapy and chemotherapy. Failure to accurately differentiate SNIP from SNIP-SCC preoperatively or intraoperatively often leads to reoperation or recurrence, significantly impacting patient outcomes. Pathological examination, clinical manifestations, and imaging features traditionally used for the early diagnosis of SNIP-SCC all have some limitations. For example, many tumors originate in the maxillary sinus, a hidden location, making histopathological biopsy challenging without general anesthesia. Additionally, the malignant transformation of SNIP may not involve the entire tumor [8–10]. Therefore, developing a novel specific tool for early SNIP-SCC diagnosis is of great clinical significance. This study utilized readily available blood markers combined with imaging data and clinical features to assist in identifying the malignant transformation of SNIP. To date, no clinical prediction model for SNIP-SCC based on tumor-related blood markers has been

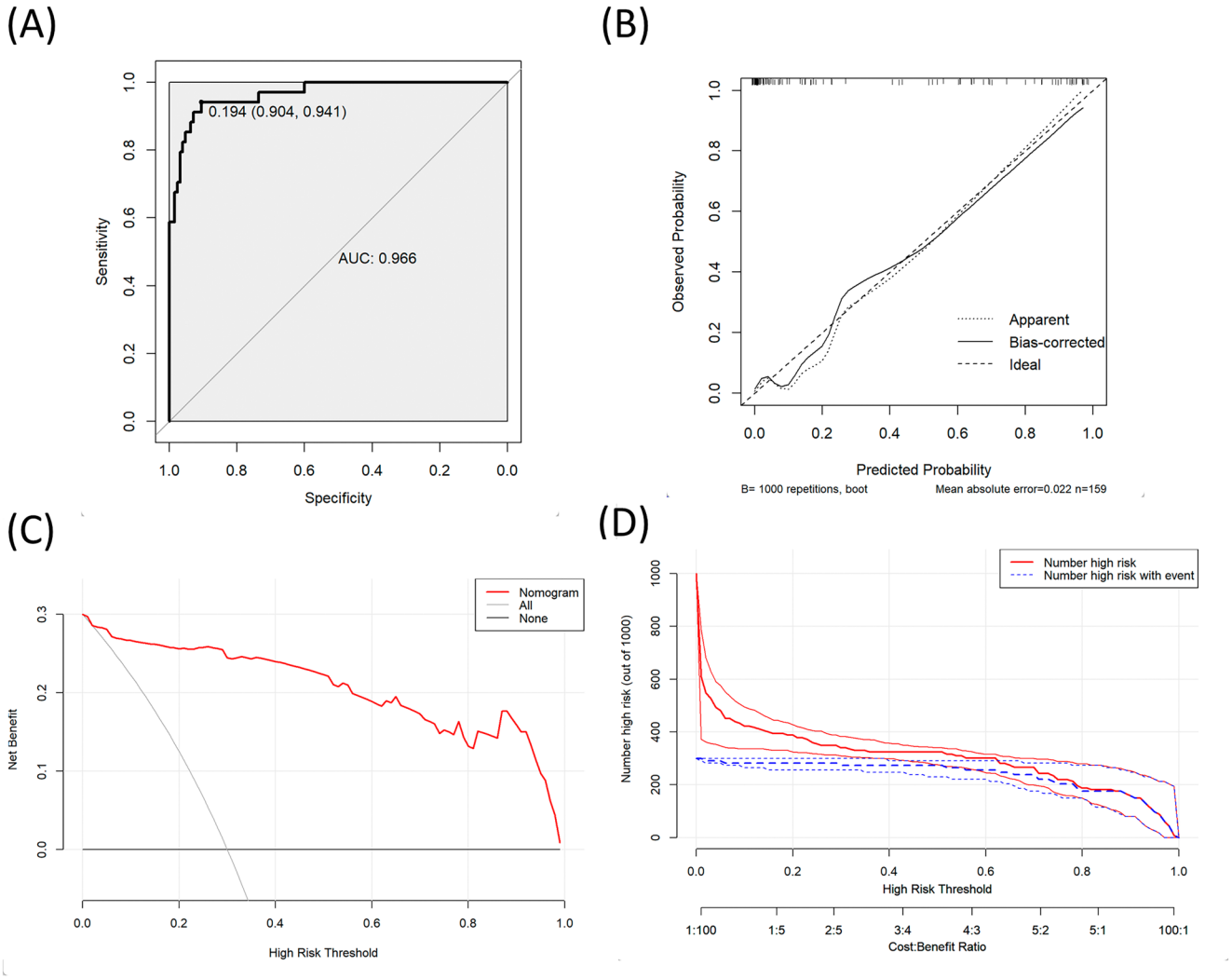


**FIGURE 2** | (A) The receiver operating characteristic curve for predicting the malignant transformation into sinonasal inverted papilloma with squamous cell carcinoma. (B) Calibration curve for predicting the malignant transformation into sinonasal inverted papilloma with squamous cell carcinoma. (C) Decision curve for predicting the malignant transformation into sinonasal inverted papilloma with squamous cell carcinoma. (D) Clinical impact curve for predicting the malignant transformation into sinonasal inverted papilloma with squamous cell carcinoma. AUC, area under the curve.

fully explored. We constructed a line graph incorporating bone destruction, CYFRA 21-1, epistaxis/blood-tinged mucus, loss of CCP, and headache/facial pain. Bone destruction was found to be the most influential factor in this model. Previous studies have demonstrated the significance of bone destruction on sinus CT in predicting SNIP-SCC. Yan and colleagues [4] found a higher likelihood of orbital wall attachment and bone destruction in SNIP-SCC. Zhang and colleagues [2] identified bone destruction in SNIP as an independent predictor of malignant transformation. However, bone destruction can also occur in benign SNIP [11–13]. The term "CCP" was proposed by Ojiri [23] to describe the characteristics of SNIP on MRI, manifested by the tumor displaying alternating high and low signal bands on T2WI and enhanced T1WI images. Further, CCP disappearance is associated with the malignant transformation of SNIP. Previous studies report that 50% of SNIP-SCC patients exhibit CCP disappearance [14–18]. Our findings are consistent with these observations, confirming bone destruction on CT and the loss of the CCP on MRI as independent predictors of malignant transformation.

The second most influential variable in the nomogram is CYFRA 21-1, a soluble fragment of cytokeratin 19. Cytokeratins are the primary components of epithelial intermediate filaments, which form part of the epithelial cell skeleton [24]. Cytokeratin 19 is an acidic type I keratin. When epithelial cells are degraded by proteolytic enzymes, soluble keratin fragments are released into the bloodstream to form CYFRA 21-1 [25]. CYFRA 21-1, a protein weighing approximately 40 kDa, was first described in 1981 by Wu et al. [26] Like other epithelial markers, only trace amounts are detectable in peripheral blood under physiological conditions [26]. Abnormally elevated serum CYFRA 21-1 levels have been reported in various cancers [27], CYFRA 21-1 has shown potential value in non-small cell lung cancer (NSCLC) diagnosis and staging, particularly squamous cell carcinoma [25, 28]. It is also valuable for predicting bladder cancer and in the prognostic monitoring of breast cancer patients after chemotherapy [29, 30]. However, its diagnostic and prognostic value in SNIP-SCC has been understudied. This study demonstrates that serum CYFRA 21-1 can be a reliable diagnostic biomarker for SNIP-SCC. In this study, SNIP-SCC patients exhibited significantly higher serum

CYFRA 21-1 levels than SNIP patients. The diagnostic cut-off value for CYFRA 21-1 was 3.51 ng/mL, with a strong predictive ability (AUC = 0.750). This suggests that CYFRA 21-1 could be valuable for diagnosing SNIP malignant transformation. These findings align with previous studies by our team [19]. Elevated serum CYFRA 21-1 in SNIP-SCC patients may be attributed to tumor cytolysis, necrosis, or potential tumor invasion and metastasis, resulting in epithelial cell destruction [30].

Headache/facial pain and epistaxis/blood-tinged mucus are additional risk factors for SNIP-SCC diagnosis. Headache/facial pain may be caused by the more aggressive inflammatory response of SNIP-SCC compared to benign SNIP. Inflammation stimulates neuropeptide release, induces histamine release from mast cells, and activates the sympathetic and parasympathetic autonomic pathways. Additionally, direct tumor invasion of adjacent nerves may lead to headache/facial pain [31, 32]. Malignant tumors are more prone to hemorrhage than benign tumors, which may explain the higher frequency of epistaxis/blood-tinged mucus.

However, although the novel diagnostic model demonstrated high sensitivity, it should not be considered a replacement for established diagnostic modalities based on clinical features. A key advantage of this model is the use of tumor-related serum markers, which are flexible, inexpensive, and widely available compared to pathological and imaging techniques. This offers rhinologists additional options for SNIP-SCC diagnosis and provides a simple, accessible tool for the initial screening of tumors in resource-limited primary care settings or for specialized patients with limitations in undergoing radiological investigations.

This study has some limitations. Firstly, the reliability of the results is compromised by its retrospective design, which increases the potential for selection bias and confounding. Additionally, patients' prognoses were not analyzed due to insufficient clinical information. Second, this was a single-center study with a small sample size, which limited the ability to conduct internal validation, potentially restricting the generalizability of the findings. Furthermore, validation in a multicenter prospective study is warranted for stronger evidence and to address these limitations.

## 3.5 | Conclusion

Our constructed line chart demonstrated that bone destruction had the highest predictive value, followed by loss of CCP, CYFRA 21-1, headache/facial pain, and epistaxis/blood-tinged mucus. In the final evaluation, the nomogram were found to have high accuracy and good clinical utility, making them valuable tools for clinicians as a reference for clinical decision-making.

**Acknowledgments**

This work was supported by grants from the Program for National Natural Science Foundation of China (81770978).

**Conflicts of Interest**

The authors declare no conflicts of interest.

**References**

1. C. T. Melroy and B. A. Senior, "Benign Sinonasal Neoplasms: A Focus on Inverting Papilloma," *Otolaryngologic Clinics of North America* 39, no. 3 (2006): 601–617.

2. L. Zhang, G. Fang, W. Yu, B. Yang, C. Wang, and L. Zhang, "Prediction of Malignant Sinonasal Inverted Papilloma Transformation by Preoperative Computed Tomography and Magnetic Resonance Imaging," *Rhinology* 58, no. 3 (2020): 248–256.

3. S. Mirza, P. J. Bradley, A. Acharya, M. Stacey, and N. S. Jones, "Sinonasal Inverted Papillomas: Recurrence, and Synchronous and Metachronous Malignancy," *Journal of Laryngology and Otology* 121, no. 9 (2007): 857–864.

4. C. H. Yan, C. C. L. Tong, M. Penta, et al., "Imaging Predictors for Malignant Transformation of Inverted Papilloma," *Laryngoscope* 129, no. 4 (2019): 777–782.

5. Q. Z. Liang, D. Z. Li, X. L. Wang, H. Huang, Z. G. Xu, and Y. H. Wu, "Survival Outcome of Squamous Cell Carcinoma Arising From Sinonasal Inverted Papilloma," *Chinese Medical Journal* 128, no. 18 (2015): 2457–2461.

6. Y. Li, C. Wang, R. Wang, et al., "Survival Outcomes and Prognostic Factors of Squamous Cell Carcinomas Arising From Sinonasal Inverted Papillomas: A Retrospective Analysis of 120 Patients," *International Forum of Allergy & Rhinology* 9, no. 11 (2019): 1367–1373.

7. W. Lawson, M. R. Kaufman, and H. F. Biller, "Treatment Outcomes in the Management of Inverted Papilloma: An Analysis of 160 Cases," *Laryngoscope* 113, no. 9 (2003): 1548–1556.

8. R. Peng, A. Thamboo, G. Choby, Y. Ma, B. Zhou, and P. H. Hwang, "Outcomes of Sinonasal Inverted Papilloma Resection by Surgical Approach: An Updated Systematic Review and Meta-Analysis," *International Forum of Allergy & Rhinology* 9, no. 6 (2019): 573–581.

9. A. Karligkiotis, D. Lepera, L. Volpi, et al., "Survival Outcomes After Endoscopic Resection for Sinonasal Squamous Cell Carcinoma Arising on Inverted Papilloma," *Head & Neck* 38, no. 11 (2016): 1604–1614.

10. M. W. Han, B. J. Lee, Y. J. Jang, and Y. S. Chung, "Clinical Value of Office-Based Endoscopic Incisional Biopsy in Diagnosis of Nasal Cavity Masses," *Otolaryngology and Head and Neck Surgery* 143, no. 3 (2010): 341–347.

11. T. Miyazaki, Y. Haku, A. Yoshizawa, et al., "Clinical Features of Nasal and Sinonasal Inverted Papilloma Associated With Malignancy," *Auris, Nasus, Larynx* 45, no. 5 (2018): 1014–1019.

12. A. Chawla, J. Shenoy, K. Chokkappan, and R. Chung, "Imaging Features of Sinonasal Inverted Papilloma: A Pictorial Review," *Current Problems in Diagnostic Radiology* 45, no. 5 (2016): 347–353.

13. P. M. Som, W. Lawson, and M. W. Lidov, "Simulated Aggressive Skull Base Erosion in Response to Benign Sinonasal Disease," *Radiology* 180, no. 3 (1991): 755–759.

14. D. M. Yousem, D. W. Fellows, D. W. Kennedy, W. E. Bolger, H. Kashima, and S. J. Zinreich, "Inverted Papilloma: Evaluation With MR Imaging," *Radiology* 185, no. 2 (1992): 501–505.

15. H. Ojiri, M. Ujita, S. Tada, and K. Fukuda, "Potentially Distinctive Features of Sinonasal Inverted Papilloma on MR Imaging," *American Journal of Roentgenology* 175, no. 2 (2000): 465–468.

16. G. Fang, H. Lou, W. Yu, et al., "Prediction of the Originating Site of Sinonasal Inverted Papilloma by Preoperative Magnetic Resonance Imaging and Computed Tomography," *International Forum of Allergy & Rhinology* 6, no. 12 (2016): 1221–1228.

17. T. Y. Jeon, H. J. Kim, S. K. Chung, et al., "Sinonasal Inverted Papilloma: Value of Convoluted Cerebriform Pattern on MR Imaging," *American Journal of Neuroradiology* 29, no. 8 (2008): 1556–1560.

18. Z. Zhang, L. Yu, J. Jiang, et al., "Development and Validation of a Clinical Prediction Model to Diagnose Sinonasal Inverted Papilloma

Based on Computed Tomography Features and Clinical Characteristics," *Ear, Nose, & Throat Journal* 20 (2022): 01455613221134421.

19. Z. Zhang, B. Xu, L. Wang, et al., "Diagnostic Value of Serum Squamous Cell Carcinoma Antigen and Cytokeratin Fragment Antigen 21-1 for Sinonasal Inverted Papilloma: An Exploratory Study," *Rhinology* 8 (2024): 351–361.

20. L. Liu, W. Xie, P. Xue, Z. Wei, X. Liang, and N. Chen, "Diagnostic Accuracy and Prognostic Applications of CYFRA 21-1 in Head and Neck Cancer: A Systematic Review and Meta-Analysis," *PLoS One* 14, no. 5 (2019): e0216561.

21. L. Zitvogel, F. Pietrocola, and G. Kroemer, "Nutrition, Inflammation and Cancer," *Nature Immunology* 18, no. 8 (2017): 843–850.

22. A. H. Mirza, G. Thomas, C. H. Ottensmeier, and E. V. King, "Importance of the Immune System in Head and Neck Cancer," *Head & Neck* 41, no. 8 (2019): 2789–2800.

23. L. Savy, G. Lloyd, V. J. Lund, and D. Howard, "Optimum Imaging for Inverted Papilloma," *Journal of Laryngology and Otology* 114, no. 11 (2000): 891–893.

24. R. Moll, W. W. Franke, D. L. Schiller, B. Geiger, and R. Krepler, "The Catalog of Human Cytokeratins: Patterns of Expression in Normal Epithelia, Tumors and Cultured Cells," *Cell* 31, no. 1 (1982): 11–24.

25. J. L. Pujol, J. Grenier, J. P. Daurès, A. Daver, H. Pujol, and F. B. Michel, "Serum Fragment of Cytokeratin Subunit 19 Measured by CYFRA 21-1 Immunoradiometric Assay as a Marker of Lung Cancer," *Cancer Research* 53, no. 1 (1993): 61–66.

26. Y. J. Wu and J. G. Rheinwald, "A New Small (40 Kd) Keratin Filament Protein Made by Some Cultured Human Squamous Cell Carcinomas," *Cell* 25, no. 3 (1981): 627–635.

27. D. Rastel, A. Ramaioli, F. Cornillie, and B. Thirion, "CYFRA 21-1, a Sensitive and Specific New Tumour Marker for Squamous Cell Lung cancer. Report of the First European Multicentre Evaluation. CYFRA 21-1 Multicentre Study Group," *European Journal of Cancer* 30A, no. 5 (1994): 601–606.

28. B. Wieskopf, C. Demangeat, A. Purohit, et al., "Cyfra 21-1 as a Biologic Marker of Non-Small Cell Lung Cancer. Evaluation of Sensitivity, Specificity, and Prognostic Role," *Chest* 108, no. 1 (1995): 163–169.

29. S. Jeong, Y. Park, Y. Cho, Y. R. Kim, and H. S. Kim, "Diagnostic Values of Urine CYFRA21-1, NMP22, UBC, and FDP for the Detection of Bladder Cancer," *Clinica Chimica Acta* 414 (2012): 93–100.

30. R. Molina, X. Filella, J. M. Augé, et al., "CYFRA 21.1 in Patients With Cervical Cancer: Comparison With SCC and CEA," *Anticancer Research* 25, no. 3A (2005): 1765–1771.

31. A. D. L. Jayawardena and R. Chandra, "Headaches and Facial Pain in Rhinology," *American Journal of Rhinology & Allergy* 32, no. 1 (2018): 12–15.

32. J. Robblee and K. A. Secora, "Debunking Myths: Sinus Headache," *Current Neurology and Neuroscience Reports* 21, no. 8 (2021): 42.